Cislunar tracking and orbital projection of Artemis I using small aperture telescope

W.J. Mandeville
Gim Der, Tim McLaughlin, Roger Mansfield, Vince Vella
InTrack Radar Technologies

ABSTRACT

We report the real-world end-to-end tracking of a cislunar satellite using a small aperture telescope. The goal of this research was to assess the ability of using a modest, commercially available telescope and camera to monitor and maintain custody of a cislunar object operating in a complex orbit. We show the quality of our observations in a variety of orbital regimes, combined with custom three-body propagation algorithms, result in orbital determination accurate enough to cue a two-degree field-of-view telescope days later.

1. INTRODUCTION

Satellites operating in non-Earth-centric orbits are becoming more prevalent. Most Space Domain Awareness (SDA) sensors and algorithms are optimized to detect and track traditional, Earth-centric satellites. These SDA tools are not well suited to track non-Earth-centric satellites and propagate their orbits. Thus, it is important to develop tools and techniques to enable the SDA community to track and maintain custody of satellites operating in these non-traditional orbits. In this paper we present data collected on NASA's Artemis I capsule and discuss the results of using custom orbital propagation algorithms to determine and propagate a cislunar orbit.

The motivation of this research performed by InTrack Radar Technologies (IRT) is to explore the potential use of a low-cost, small-aperture telescope to acquire and track an object in a non-traditional, cislunar orbit, and to use the data to assess the performance of new three-body orbital determination algorithms developed by DerAstrodynamics.

In this paper, we present data and analysis showing the accuracy of our observations as well as the accuracy and durability of the orbital determination and propagated orbit using three-body orbital algorithms. Our conclusion is that a modest telescope with capable command and control techniques, coupled with cutting-edge three-body orbital algorithms will do a creditable job acquiring, tracking, and maintaining custody of cislunar objects like the Orion crew capsule.

2. EXPERIMENTAL APPARATUS

The observation data for this research was collected at IRT's Pine Park Observatory (PPO) located near Colorado Springs, Colorado. The telescope used was a Celestron 8" f/2.0 Rowe-Ackermann Schmidt Astrograph (RASA) coupled with a QHY 174M-GPS camera. Figure 1 shows the observatory and three telescopes within. The telescope on the right is the 8" Celestron used to track Artemis I for this research. Both the telescope and the camera are consumer grade and commercially available. The telescope combined with the QHY 174M-GPS camera's 11.25 x 7.03 mm CMOS focal plane provides a 1.6 x 1.0 degree field-of-view. PPO uses custom developed telescope control and satellite tracking software.

The telescope control software drives the telescope in sidereal and rate-track modes when collecting observations on typical Earth-orbiting satellites. The telescope pointing locations are determined using orbital element sets such as Three Line Elementsets (TLEs), which are downloaded from space-track.org. When observations are collected in sidereal mode, the stars appear stationary while the satellite appears as a streak. Conversely, in rate-track mode, the stars will appear as streaks while the satellite appears as a stationary dot. When tracking cislunar objects like Artemis I, the telescope can be pointed using ephemerides data. When tracking distant objects like Artemis, the slow relative motion against the background stars causes images to have stars as well as the satellite show up as non-streaking

Fig. 1: Pine Park Observatory is a roll off shed design housing three telescopes. The telescope furthest to the right is the 8" Celestron used for the experimentation reported in this paper.

point sources. Images are processed automatically using Source Extractor[2] to locate the background stars. Once the background stars are mapped, the star locations are passed to a local instantiation of Astronomy.net[7] for astrometric processing. The astrometric processing corrects for optical distortions and enables very accurate right ascension and declination measurements for satellite and star locations. The star catalog used by Astrometry.net for the data presented in this paper was the UCAC4 catalog[8]. Once the background stars have been mapped, the position of the satellite can be accurately determined relative to the mapped stars.

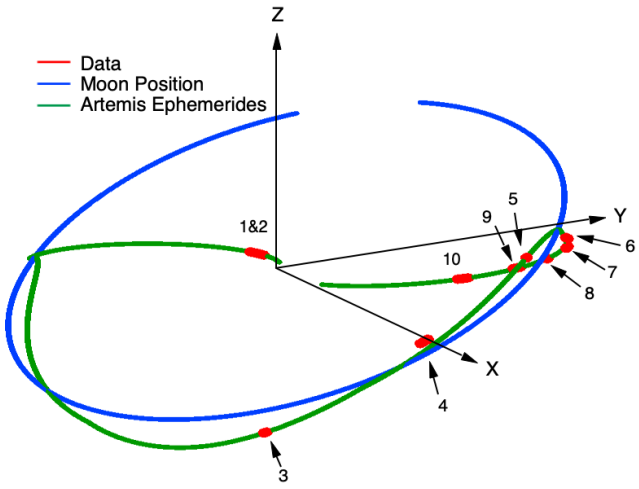

Fig. 2: Artemis orbital path is shown in green in Earth-centered coordinates. Red indicates where data observations were collected by Pine Park Observatory, while blue is the moon's orbital path.

To acquire and track the Orion crew capsule shortly after launch, the research team used JPL Horizons[6] ephemeris data. However, since the launch was later than planned, the ephemeris data was incorrect. The research team searched around the location where Artemis was supposed to be and successfully located the rocket body and crew capsule approximately 45 minutes ahead of the projected location. The need to perform a time consuming search, even when ephemerides are provided on a cooperative satellite, highlights the difficulty of maintaining custody on a satellite in a complex orbit. The research team repeated the process nine more times, over the 25-day mission, using the JPL Horizons ephemerides for initial pointing followed by an area search, when necessary, to find and track the crew capsule. The captured images were processed photometrically using aperture photometry and astrometrically using custom software that utilizes Astrometry.net and a UCAC4 star catalog. The accuracy of the observations was compared to the JPL Horizons special perturbations ephemeris showing our observations to be accurate to within a few arcseconds. Figure 2 shows the orbital path of Artemis I in green and the location of all of the data collections in

red. The initial track, which occurred shortly after launch, had the rocket body as well as the Artemis crew capsule in the same field-of-view and is represented as track 1 and track 2 respectively. The rest of the tracks were of only the crew capsule.

3. ALGORITHMS

DerAstrodynamics developed custom Initial Orbit Determination (IOD), Batch Differential Correction (BDC), and orbital prediction (xBDC2_optical) algorithms suitable for processing track data on satellites. The analytic xBDC2_optical algorithm is comprised of seven optical IOD and two optical BDC algorithms[5, 4]. These algorithms were used to produce initial, final, and predicted state vectors for the Artemis I mission using the observations for all ten optical tracks. In order to process the data for this research, the algorithms were modified to efficiently propagate the trajectories with analytic Sun and Moon gravitational influences included in a three-body orbit propagation. The following paragraphs describe the algorithmic flow used to process the Artemis I tracks.

The first step is to perform an IOD. The Gauss IOD method[1] uses three observations to form an initial state vector. Figure 3a depicts the Earth-centered geometry used for IOD. The initial state vector is calculated at t_2 and then propagated back to t_1 giving $\mathbf{x}(t_1)_{IOD} = (\mathbf{r}(t_1)_{IOD}, \mathbf{v}(t_1)_{IOD})$. Once IOD at t_1 is determined, it is used as an input for the BDC algorithm. The BDC algorithm uses all of the observations in a given track to determine a final state vector at t_1 giving $\mathbf{x}(t_1)_{DC} = (\mathbf{r}(t_1)_{DC}, \mathbf{v}(t_1)_{DC})$. One of the challenges in processing these data is related to the difficulty in determining range from optical observations that only provide angle measurements. The initial state vector from IOD may be improved by using an iterative method and using the results from BDC to re-estimate the initial state vector for IOD. The efficient design of xBDC2_optical allows it to process hundreds of observations in a track very quickly while including analytic Sun and Moon perturbations.

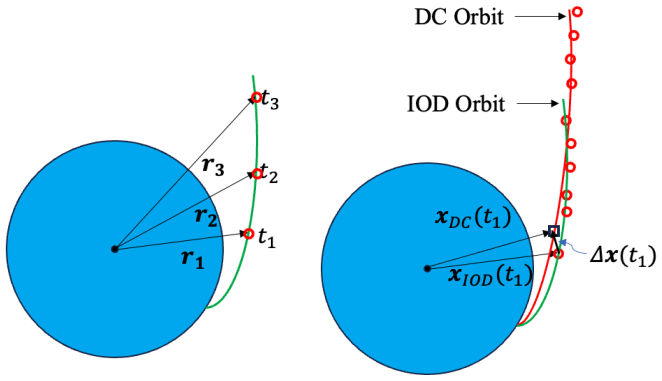

(a) Initial Orbit Determination (b) Batch Differential Correction

Fig. 3: Geometry for Initial Orbit Determination (IOD) and Batch Differential Correction (BDC) using Earth-centered coordinate system. Figure 3a depicts using three observations for the initial orbit determination, while Figure 3b depicts using all available observations to refine the initial orbit as determined by the IOD process to arrive at a new initial state vector, $\mathbf{x}_{DC}(t_1)$.

IOD and DC state vector accuracy is dependent on the quality of the observations. PPO observations on low Earth-orbit (LEO) satellites are typically under 5 arcseconds. The data collected on Artemis I varied in accuracy throughout the mission due to inherent challenges of collecting observations on a deep space object and the proximity to the bright Moon. These real-world observations from an 8" telescope provide an ideal test case for investigating the computational ability of DerAstro's algorithms to determine useful state vectors on satellites.

The state vector correction with respect to the initial state vector $\mathbf{x}(t_1)$ for BDC at epoch observation time, t_1, may be estimated as

$$\Delta\mathbf{x}(t_1) = (\mathbf{H}^T\mathbf{H})^{-1}\mathbf{H}^T(\mathbf{y}(t_i) - \hat{\mathbf{y}}(t_i)), \tag{1}$$

where $\mathbf{H} = \mathbf{H}(t_i)$ is the observation matrix and $\mathbf{y}(t_i) - \hat{\mathbf{y}}(t_i)$ is the analytic residual vector for observations $i = 1, 2, \ldots, n$.

The computation of the BDC state correction vector, $\Delta\mathbf{x}(t_1)$ in Eqn. 1 at epoch t_1 is expressed as

$$\Delta\mathbf{x}(t_i) = \mathbf{H}(t_i)\Delta\mathbf{x}(t_1) = \mathbf{O}(t_i,t_1)\Delta\mathbf{x}(t_1), \tag{2}$$

giving

$$\mathbf{H}(t_i) = \mathbf{O}(t_i)\mathbf{\Phi}(t_i,t_1), \tag{3}$$

where

$$\mathbf{O}(t_i) = \begin{bmatrix} \frac{A_x}{\rho} & \frac{A_y}{\rho} & \frac{A_z}{\rho} & 0 & 0 & 0 \\ \frac{D_x}{\rho} & \frac{D_y}{\rho} & \frac{D_z}{\rho} & 0 & 0 & 0 \end{bmatrix} \tag{4}$$

and $\mathbf{\Phi}(t_i,t_1)$ is the state transition matrix. The state correction vector for BDC, $\Delta\mathbf{x}(t_1)$, is at epoch t_1. The state transition matrix $\mathbf{\Phi}(t_i,t_1)$ is needed to connect the matrix $\mathbf{O}(t_i)$ of BDC to the observation matrix $\mathbf{H}(t_i)$ at t_i for $i = 1,2,\ldots,n$. In Eq. 4, the **A** and **D** vector component partial derivatives with respect to x, y, and z are part of the **LAD** triad of unit vectors at the target. **L** points from sensor to target. **A** lies parallel to the equatorial plane, perpendicular to **L** and the hour circle of the satellite. And finally, $\mathbf{D} = \mathbf{L} \times \mathbf{A}$. For a more comprehensive discussion of the algorithms used for this research, please see [4] and [5] which were recently presented by Dr. Der at the 2023 AAS/AIAA Astrodynamics Specialist Conference in Big Sky Montana. Additional discussion and examples are available at [3].

4. RESULTS

Seven of the ten Artemis I tracks (1, 2, 6, 7, 8, 9, 10 as depicted in Fig. 2), were successfully processed by the Gauss IOD algorithm. The results shown in Table 1 indicate very high ellipticity ($e > 0.94$) in Earth-centered inertial (ECI) coordinates which is challenging for IOD. Tracks 3, 4, and 5 are exceptionally difficult to process since they are very short arc collects while Artemis I was in distant retrograde orbit (DRO) around the Moon. Track 4 did solve with the Gauss IOD algorithm but tracks 3 and 5 did not produce reasonable state vectors. To process tracks 3 and 5, a short-arc range-solving technique was required. It is likely that a Moon-centered inertial (MCI) reference system would have worked more efficiently for the DRO cases, but code modification to work in MCI was beyond the scope of the research presented here.

Track	Time	a (km)	e	$i(deg)$	$\Omega(deg)$	$\omega(deg)$	$M(deg)$
1 (IOD)	0.0	171 354	0.9597	30.438	10.605	20.525	4.594
1 (BDC)	0.0	196 821	0.9649	30.495	10.570	21.030	3.689
2 (IOD)	0.0	106 665	0.9435	30.270	11.105	16.226	8.797
2 (BDC)	0.0	194 000	0.9644	30.263	10.967	20.686	3.765
6 (IOD)	0.0	271 247	0.9636	101.571	218.917	353.924	71.240
6 (BDC)	0.0	213 830	0.9526	102.592	218.634	348.225	137.650
7 (IOD)	0.0	204 607	0.9677	89.393	221.920	344.998	215.329
7 (BDC)	0.0	208 258	0.9643	92.518	221.228	345.313	209.105
8 (IOD)	0.0	210 810	0.9736	84.344	222.814	344.683	263.826
8 (BDC)	0.0	196 749	0.9654	88.492	222.074	347.015	225.560
9 (IOD)	0.0	218 212	0.9732	84.327	222.660	344.939	287.868
9 (BDC)	0.0	237 140	0.9741	85.658	222.489	344.081	297.238
10 (IOD)	0.0	228 153	0.9722	85.791	222.430	345.025	317.235
10 (BDC)	0.0	234 537	0.9734	85.516	222.445	344.870	319.581

Table 1: Seven Artemis-1 tracks successfully processed by Gauss IOD and BDC.

Once IOD and BDC were accomplished for all tracks, the research team used ephemerides from JPL Horizons as truth data in order to determine how accurate the orbital determination was for each track. The results for track 1 are shown in Fig. 4. The observation data plotted in Fig. 4a (blue dots) is plotted as a function of time. The predicted orbits from IOD and BDC are shown in green and red respectively. The quality of the predicted BDC orbit was assessed by

propagating the orbital prediction forward in time and measuring how long it took to drift away from the true orbit, as provided by JPL Horizons. The research team used the metric of 2 degrees as the limit for ease of reacquisition. This is based on using a telescope with a large enough field-of-view to find a satellite, using a simple search if it is within 2 degrees of the predicted location. This amount of time can be thought of as the ”durability” of the orbital prediction.

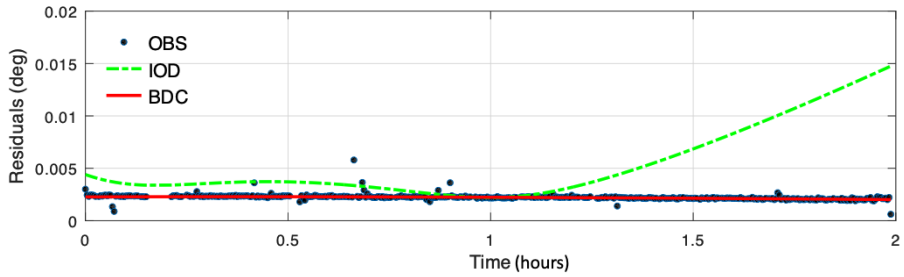

(a) Track data (OBS) and orbital determination results.

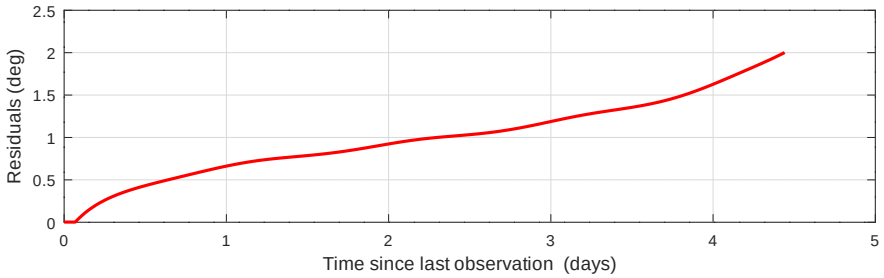

(b) Projected orbit compared with JPL Horizons truth data.

Fig. 4: Track 1 results. The upper graph shows the initial orbit in green and the batch differential corrected orbit in red as they compare to the data which is shown in blue dots. The lower graph shows how the BDC solution compares over time with the truth data from JPL for the location of Artemis I. For the case of track 1, a 2 degree field-of-view telescope could reacquire the satellite about 4.5 days later.

The durability of the orbital predictions for each of the ten tracks of Artemis I are presented in Table 2.

Track	Durability (days)
1	4.5
2	4.0
3	2.0
4	1.4
5	0.6
6	3.5
7	3.8
8	2.5
9	1.6
10	1.0

Table 2: Time following BDC that object remains within 2 degrees of true position as determined by JPL ephemerides. This represents the ”durability” of the prediction.

5. SUMMARY

The goal of this research was to assess the ability of using a modest, commercially available telescope and camera, in conjunction with custom algorithms, to monitor and maintain custody of a cislunar satellite operating in a complex orbit. This study has shown that a small aperture telescope was more than sufficient for tracking and accurately predicting the orbit of a satellite in a complex, non-Earth-centric orbit. This research highlights the value that small telescope data can bring to the space domain awareness enterprise when combined with state-of-the-art algorithms. Looking forward, these results show great promise for an inexpensive way to enhance the space domain awareness enterprise.

6. REFERENCES

[1] Roger R. Bate, Donald D. Mueller, and Jerry E. White. *Fundamentals of Astrodynamics*. Dover Publications, 1971.

[2] E. Bertin. SExtractor: Software for source extraction. *Astronomy and Astrophysics Supplement Series*, 117(2):393–404, 1996.

[3] G.J. Der. *Astrodynamics Algorithms for Rapid Space Catalog Building*. Der Astrodynamics, Texas, USA, October 2021. `https://www.derastro.com`.

[4] G.J. Der. Differential correction algorithms for rapid optical and radar data processing. In *AAS/AIAA Astrodynamics Specialist Conference*, August 2023.

[5] G.J. Der. Initial orbit determination algorithms for rapid optical and radar data processing. In *AAS/AIAA Astrodynamics Specialist Conference*, August 2023.

[6] Jet Propulsion Laboratory. JPL Horizons on-line solar system data and ephemeris computation service. `https://ssd.jpl.nasa.gov/horizons/`. Accessed Nov 16, 2022 to Dec 11, 2022.

[7] Dustin Lang, David W. Hogg, Keir Mierle, Michael Blanton, and Sam Roweis. Astrometry.net: Blind astrometric calibration of arbitrary astronomical images. *Astronomical Journal*, 139(5):1782–1800, 2010.

[8] N. Zacharias, C. Finch, T. Girard, A. Henden, J. L. Bartlett, D. G. Monet, and M. I. Zacharias. The Fourth US Naval Observatory CCD Astrograph Catalog (UCAC4). *VizieR Online Data Catalog*, 1322, November 2013.